Electrical Power and Energy Systems 170 (2025) 110884

Contents lists available at ScienceDirect

International Journal of Electrical Power and Energy Systems

journal homepage: www.elsevier.com/locate/ijepes

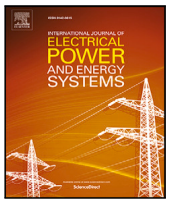

Under frequency load shedding aware unit commitment in island power systems

Miad Sarvarizadeh [a,*], Mohammad Rajabdorri [a], Enrique Lobato [a], Lukas Sigrist [a], Behzad Kazemtabrizi [b], Matthias Troffaes [c]

[a] IIT, Comillas Pontifical University, Spain
[b] Department of Engineering, Durham University, UK
[c] Department of Mathematical Sciences, Durham University, UK

ARTICLE INFO

Keywords:
Under-frequency load-shedding
Unit commitment
Island power systems
Machine learning
Logistic regression
Regression tree

ABSTRACT

The transition from fossil fuels to renewable energy sources in power systems has resulted in lower system inertia and deteriorated frequency response characteristics. The challenge becomes even more pronounced in island power systems, where low inertia and limited frequency control capacity are already issues. Despite the existing preventive measures to maintain frequency limits, under-frequency load-shedding (UFLS) remains a crucial corrective action. In small isolated power systems, even with high amounts of reserve, big outages will lead to inevitable UFLS due to scarcity of inertia and primary frequency control capacity. Using a data-driven regression tree method, this paper introduces a novel UFLS-aware unit commitment formulation that can accurately estimate the amount of resulting UFLS for every possible outage. The estimations are then utilized to relax the reserve requirement constraint and lower the operation costs. The proposed formulation enables co-optimizing operation costs and UFLS to minimize the total cost. Additionally, the response speed of generating units is considered, ensuring timely reserve delivery. The efficacy of the proposed method is demonstrated through simulations on the model of a Spanish island power system, highlighting potential reductions in operation costs and system security improvements.

1. Introduction

Given the environmental impacts of fossil fuels and the decreasing capital costs of renewable energy sources (RES) [1], many power systems are transitioning towards RES instead of relying solely on thermal generators. However, this shift has led to lower inertia and deteriorated frequency response characteristics in power systems, as RES may not inherently provide inertia [2]. This issue is particularly critical in island power systems (IPS), which are already suffering from low inertia [3]. The smaller scale of IPS means fewer generating units are connected, resulting in lower system inertia and overall frequency control capacity. Moreover, since each generating unit represents a significant portion of the total demand, the loss of even a single unit can lead to a rapid frequency drop. Without timely system-wide frequency protections, this drop could trigger a cascading failure, ultimately leading to a blackout.

Operation planning in IPS is primarily centralized, with the system operator sequentially performing unit commitment (UC) across various time horizons. Traditional UC approaches often overlook frequency considerations. Frequency stability can be incorporated into the UC within the framework of security constrained unit commitment (SCUC) and more specifically, frequency constrained unit commitment (FCUC). Three main frequency indicators, including rate of change of frequency (RoCoF), frequency nadir, and quasi-steady-state frequency, could be constrained to a certain threshold after disturbance to ensure the power grid frequency stability [4]. Consequently, convex frequency constraints concerning these indicators are derived utilizing analytical or data-driven methods to form an FCUC formulation [5–13]. [5] presents an FCUC using analytically derived constraints that limit post-contingency steady-state frequency, transient area frequencies, tie-flow deviations, and RoCoF of two-area power systems. The pseudo-Boolean function theorem has been used to linearize the nadir functions.

In [6], an accurate approximation of the differential–algebraic equations that describe the power system is presented using Bernstein polynomials. First, the differential equations are converted into a system of linear equations, which is then implemented in the UC. By taking advantage of the properties of Bernstein polynomials, appropriate constraints are derived from the dynamic response solution. A RoCoF-constrained location-based UC formulation is presented in

* Corresponding author.
E-mail address: msarvarizadeh@comillas.edu (M. Sarvarizadeh).

https://doi.org/10.1016/j.ijepes.2025.110884
Received 10 March 2025; Received in revised form 30 May 2025; Accepted 5 July 2025
Available online 23 July 2025

Nomenclature

Indices and sets

ℓ	Index of the lost unit (alias index of generators)
$\mathcal{L}$	Set of all resulting leaves
$\mathcal{T}$	Set of all time intervals
i	Index of generators
J	Set of all features
j	Index of features
L	Index of the leaves
s	Alias index for time intervals
t	Index of time intervals

Parameters

α_j	Linear regression coefficients
β_j	Logistic regression coefficients
$\mathcal{D}_t$	Demand at time t [MW]
$\mathcal{H}_i$	Inertia constant of unit i [s]
DT	Minimum down-time of generators [hours]
FOR	Forced outage rate of generators [%]
UT	Minimum up-time of generators [hours]
C^o	Post-outage cost of UFLS [€]
C_{th}	Threshold of splitting nodes in tree structure
D	Load damping factor
f_0	Nominal frequency [Hz]
g_t^s	Solar generation at time t [MW]
g_t^w	Wind generation at time t [MW]
K_i	Turbine-governor gain of unit i
M	A sufficiently big positive number
$P_i^{\max}$	Maximum power output of unit i [MW]
$P_i^{\min}$	Minimum power output of unit i [MW]
R_i^{down}	Maximum ramp-down of unit i [MW]
R_i^{up}	Maximum ramp-up of unit i [MW]
S_i^{base}	Base power of unit i [s]
T	Delivery time of units [s]
$\hat{K}_i$	Turbine-governor gain of unit i divided by its T

Variables

c^{UFLS}	UFLS costs [€]
c^{g}	Generation costs [€]
c^{suc}	Start-up costs [€]
H_ℓ	Weighted summation of inertia constants of online units after outage of unit ℓ [s.MW]
p	Power variable [MW]
$p_{\ell,t}^{\text{UFLS}}$	Amount of UFLS after outage of unit ℓ at time t [MW]
$p_{\text{SFR}}^{\text{UFLS}}$	UFLS calculated using SFR model
p_ℓ	Power lost after outage of unit ℓ [MW]
R_ℓ	Sum of available reserve after outage of unit ℓ [MW]
$r_{i,t}$	Reserve provided by unit i at time t [MW]
u	Commitment variable
v	Start-up variable
w	Shut-down variable
z_L	Leaf membership binary variable

[7] that focuses on differentiating frequency characteristics based on location. Also, the economic effects of virtual inertia are explored. The proposed formulation is then linearized using piece-wise linearization methods. In [8] an analytical approach to model frequency stability constraints considering frequency response from RES is proposed. Detailed governor dynamics are included. The proposed FCUC is formulated as an mixed integer non-linear programming (MINLP) problem and then solved using decomposition techniques. A multi-stage stochastic FCUC problem is presented in [9] that incorporates a dynamic simulation model of frequency response in the third stage of the problem and considers deloading of RES. A nested Benders decomposition algorithm is then proposed to solve the problem. Authors in [10] investigated the diversities in the frequency response of conventional and inverter-based generators and proposed a robust FCUC formulation.

In [11], a data-driven method based on support vector machines is proposed to convexify the frequency nadir constraint. An FCUC model formulated as a mixed-integer quadratic programming problem is provided. A conservative sparse neural network method is proposed in [12] that approximates frequency nadir and step-wise constraints. Then a mixed integer linear programming (MILP) representation of these constraints is given using the big-M method and added to the conventional UC problem. In [13], an extreme learning machine model is proposed to get a linearized frequency nadir constraint. Also, the droop gains of available generators are optimized in the day-ahead UC problem. A distributionally robust FCUC framework is proposed in [14] that employs support vector machine decision trees to model the nonlinear frequency nadir constraint as linear constraints. In [15], a frequency-constrained stochastic look-ahead power dispatch model is proposed that optimally schedules the virtual inertia and droop coefficients of RES and energy storage systems to ensure frequency stability under uncertainty. The study modeled RES uncertainties using a Gaussian mixture model and linearized the frequency nadir constraint using a convex hull approximation.

All the studies mentioned above are based on preventive measures that ensure the frequency remains within limits in every possible contingency under different operating conditions without taking any post-contingency corrective action. On the other hand, corrective measures such as UFLS are employed as a last resort to accelerate frequency response recovery [16]. UFLS is automatically activated based on the measurements and predefined schemes. One way of categorizing different UFLS schemes is by dividing them into conventional, semi-adaptive, and adaptive, based on the level of flexibility they exhibit and the ability to adapt to the system operating condition at a particular time [17]. Conventional UFLS schemes involve triggering protection relays to disconnect predefined portions of the load according to a priority list in a multi-stage manner when the frequency falls below certain thresholds and for a specified duration [18]. Researchers have presented several conventional UFLS schemes. In [19] a probabilistic scheme that considers the inertia time constant, load damping, and generation deficiency uncertainties are presented. A load priority method is presented in [20] that gives the proposed scheme some flexibility to optimize the amount of shed load. A robust optimal design of the conventional UFLS scheme is presented in [21]. This study utilizes a synthetically generated dataset to tune the UFLS settings of existing UFLS schemes. Conventional schemes cover the vast majority of UFLS schemes currently in use worldwide.

Semi-adaptive schemes can partially adjust the load-shedding process, i.e., based on RoCoF. However, the UFLS relay settings are still determined through simulations and experience. [22] presents a RoCoF based semi-adaptive scheme, where the magnitude of load shedding in each step is evaluated offline based on simulation results and experience of the operational engineers. An approach to apply the RoCoF information in the UFLS scheme design is presented in [23]. In this UFLS scheme, different amounts of shedding load have been assigned to each integrating RoCoF value range at each UFLS step.

Adaptive schemes can fully adjust the load-shedding process to operating conditions [24–27]. These schemes typically are centrally controlled, based on locally acquired estimates of frequency, RoCoF, and voltage amplitude transmitted by wide-area measurement systems or Supervisory control and data acquisition, as well as on estimates of the magnitude of the disturbance by the swing equation [17]. However, adaptive UFLS schemes do not necessarily need to be centralized, yet still provide a high level of efficiency and flexibility [28].

In real-world IPS applications, conventional schemes are predominantly used because adaptive methods typically require efficient and fast communication channels to monitor measurements and estimate power imbalances, which are currently unavailable in practice. Additionally, constant variations of RoCoF make it difficult to implement advanced UFLS schemes [29].

The majority of the literature focuses on containing the post-contingency frequency response so that the UFLS scheme is never activated. In [30], a data-driven framework based on deep neural networks is presented to predict frequency nadir and embedded into MILP formulations. The proposed model selects samples with frequency nadirs close to the UFLS threshold, to improve the model's performance and prevent UFLS. [31] proposes a scheme that coordinates UFLS with ancillary services to prevent unnecessary load shedding. This study utilizes the data captured by phasor measurement units and power injection to arrest the frequency decay.

To the best of our knowledge, very few studies have explored the idea of incorporating UFLS into the scheduling formulations and analyzing its potential economic effects. In small IPS with low amounts of inertia available, this would be more relevant as big outages will lead to inevitable UFLS events. An analytical nadir constraint that secures thermal units' inertia and frequency response to be higher than a constant is presented in [32]. This formulation yields a nonlinear expression. Blocks of UFLS are considered with one nadir constraint per block. Then the optimal amount of UFLS is chosen, assuming a linear generation increase in time, and a known outage size. A frequency constrained contingency analysis (FC-CSA) model is proposed in [33] that incorporates UFLS in the primary frequency response. Subsequently, a refined system frequency response (SFR) model is derived and represented by MILP constraints. However, the model primarily focuses on contingency state analysis and does not explore different commitment states based on UFLS. Additionally, this study does not investigate the economic consequences of UFLS.

In [34] an analytical method based on second-order cone approximation is presented to obtain a convexified frequency nadir constraint that incorporates UFLS. Additionally, the potential economic effects of incorporating UFLS are explored in their study. Authors in [35] provide an analytical method to include UFLS as a corrective measure to the UC problem, forming a corrective frequency constrained unit commitment (C-FCUC) formulation. Unlike the approaches in [34,35], in this paper the real UFLS schemes used in most IPSs, which are step-wise and nonlinear, are modeled by utilizing data-driven methods. Fig. 1 gives a timeline of the reviewed references, indicating different approaches in the literature.

In the case of IPS and sufficiently large outages, the UFLS is inevitable because every generating unit contributes to a big portion of the total generation. It is important to note that in IPS, simply having enough reserves is not enough to prevent UFLS. When an outage occurs, the frequency drops so rapidly that UFLS schemes are triggered before the remaining units have a chance to restore balance. Also, trying to prevent UFLS entirely by setting conservative frequency nadir thresholds would not be feasible in small IPS [36]. By incorporating the modeling of UFLS into the UC problem, it is possible to leverage the unavoidable occurrences of UFLS to reduce the reserve requirement and potentially the operation costs. This suggests that holding back less spinning reserve is justified, given that UFLS events occur anyway, and system security is not jeopardized. The real UFLS schemes used in an island in Spain, which are step-wise and contain preset time delays in triggering the relays, are used to estimate UFLS, utilizing a data-driven approach based on regression trees in [37]. The proposed data-driven approach has several advantages compared to other common regression models, including higher accuracy than linear regression and far less complexity than typical decision tree regressor models. This has been demonstrated in detail in the following sections. This paper uses the UFLS estimation of [37], and implements it in the UC problem, to form a novel UFLS-aware UC formulation capable of reducing the operation costs of the investigated system.

Following the incorporation of UFLS into the UC formulation, the primary frequency response must be modified so that the remaining net power imbalance following a shortfall will be distributed among the online units according to their speed of response. The current formulations do not acknowledge the generating units' response speed, although a common assumption when calculating the frequency nadir analytically is that all the units can deliver their headroom in a constant amount of time (for example, 10 s is commonly used). In this paper, generating units' response speed is considered to ensure that units are fast enough to deliver their headroom as intended. Table 1 gives a comparison between the most related papers in the literature and this paper. In Table 1, the term "real scheme" refers to the current conventional scheme that is implemented in the operation of the island power system of the case study. The current schemes are deterministic, they act by shedding a predetermined amount of consumption at predetermined frequency thresholds after predetermined time delays [17]. The problem of estimating the amounts of shed load through the current schemes is more complicated since the relationship between the final amount of shed load and the decision variables in the scheduling problem is not clear. To address this problem, a data-driven model that captures the complicated relationship with MILP constraints is proposed. The term "real scheme" is used here to differentiate between the currently implemented conventional scheme modeled here and the adaptive schemes proposed in the literature, but have not been implemented in the operation of the island power system yet.

The main contributions of this paper are presented as follows:

- We argue that having an estimation of the amount of UFLS in the scheduling process is beneficial, as big outages in small IPS will eventually lead to inevitable UFLS occurrences. Therefore, we propose a UFLS-aware UC formulation by incorporating the UFLS estimation in the UC problem. For the UFLS estimation, we use the data-driven regression tree method presented in [37].
- The linearized estimation of UFLS is used as a source of reserve in the proposed formulation, which leads to cost reduction.
- The generating units' response speed is acknowledged, ensuring that each unit will provide its reserve in time. An acceleration strategy solution tailored to the model's characteristics is presented to implement the required constraint more effectively.
- The proposed formulation is studied using the model of a real island power system in Spain and reflects the real UFLS schemes that are currently used in the Spanish islands. Various UFLS costs and days in each season are analyzed to demonstrate the capability of the proposed formulation.

The remainder of this paper is organized as follows: first, in Section 2, the proposed UFLS-aware formulation, and the data-driven approach to estimate UFLS are described. Section 3 describes the investigated system, the training process of the regression tree structure, and the numerical results. Finally, Section 4 provides the conclusions.

2. Methodology

In this section, the proposed methodologies are discussed. In Section 2.1, the UC formulations are presented, and the proposed UFLS-aware UC is explained. Section 2.2 presents the UFLS estimation procedure and the utilized tree structure. Linear constraints representing

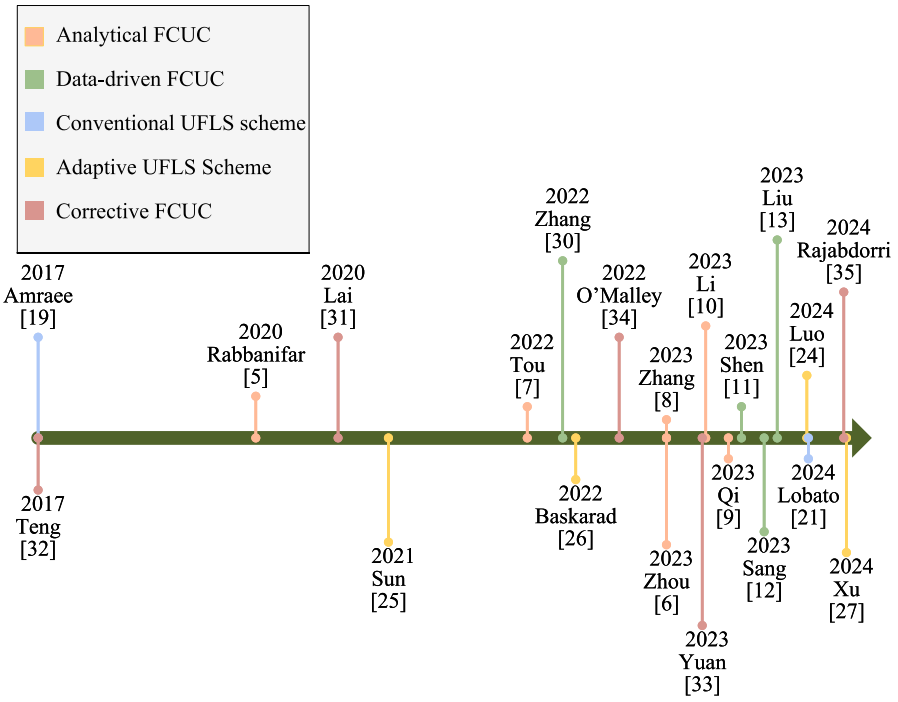

Fig. 1. Timeline of the reviewed papers.

Table 1
Comparison of the most related papers.

Paper	Formulation		UFLS model		Case Study
[32]	stochastic FCUC with UFLS modeling	unit response speed not considered	adaptive scheme	analytical	modified Great Britain 2030
[33]	FC-CSA with UFLS modeling	unit response speed not considered	adaptive scheme	analytical	modified IEEE 6-bus and IEEE 118-bus
[34]	FCUC with UFLS modeling	unit response speed not considered	adaptive scheme	analytical	Great Britain 2030
[35]	FCUC with UFLS modeling	with unit response speed	adaptive scheme	analytical	Real Spanish Island
this paper	UFLS-aware UC	with unit response speed	real scheme	data-driven	Real Spanish Island

the tree structure are derived and added to the UFLS-aware UC formulation. Finally, in Section 2.3, models to be analyzed are presented and compared. Fig. 2 presents a flowchart of the overall methodology framework of the paper.

2.1. UFLS-aware UC formulation

Typically, a MILP problem is formulated to solve the day-ahead scheduling problem of power systems, minimizing the operation costs. The UC formulation is presented below.

Objective function. Let $p_{i,t}$ and $u_{i,t}$ respectively denote the power output and commitment status of unit i at time t.

By p we denote the vector of $p_{i,t}$ across all units and time points, and similarly for u. The objective of the UC problem is to find the p and u that minimize the operation cost. This cost comprises the sum of generation cost $c^{g}(p)$ and start-up costs $c^{suc}(u)$. Thus, the overall objective is

$$\min_{u,p} \; c^{g}(p) + c^{suc}(u) \tag{1}$$

The generation cost $c^{g}(p)$ is usually a quadratic function of the power p, which will be piece-wise linearized so that we can use it in the MILP formulation. The start-up cost $c^{suc}(u)$ depends on how much time has passed since the unit was last running. If the unit is still hot, less energy is needed to heat the boiler, hence, the start-up cost is lower. This paper uses an 8-step start-up cost function inspired by [38].

Although the UFLS incurs significant costs, large outages are rare. Nevertheless, UFLS can significantly alleviate the reserve required. To effectively manage these contrasting impacts and optimize the UFLS alongside the operation costs, the expected cost of UFLS must be determined by multiplying the post-outage cost of UFLS by the probability of the outage occurring [34]. The expected cost of UFLS is added directly to the objective function. So Eq. (1) will be rewritten as below,

$$\min_{u,p} \; c^{g}(p) + c^{suc}(u) + c^{UFLS}(p^{UFLS}) \tag{2}$$

where p^{UFLS} is the vector of all possible UFLS occurrences. This refers to every possible UFLS activation following the outage of each generating unit that is on and could suffer an outage. This includes the summation of all of the activated UFLS stages for all possible contingencies. The term $c^{UFLS}(.)$ is calculated as,

$$c^{UFLS}(p^{UFLS}) = \sum_{t} \sum_{\ell} C^{o} \times \mathrm{FOR}_{\ell} \times p^{UFLS}_{\ell,t} \tag{3}$$

where ℓ is an alias index of generating units denoting the lost unit, C^{o} is the post-outage cost of UFLS in €/MW, and FOR is the forced outage rate of generators in %.

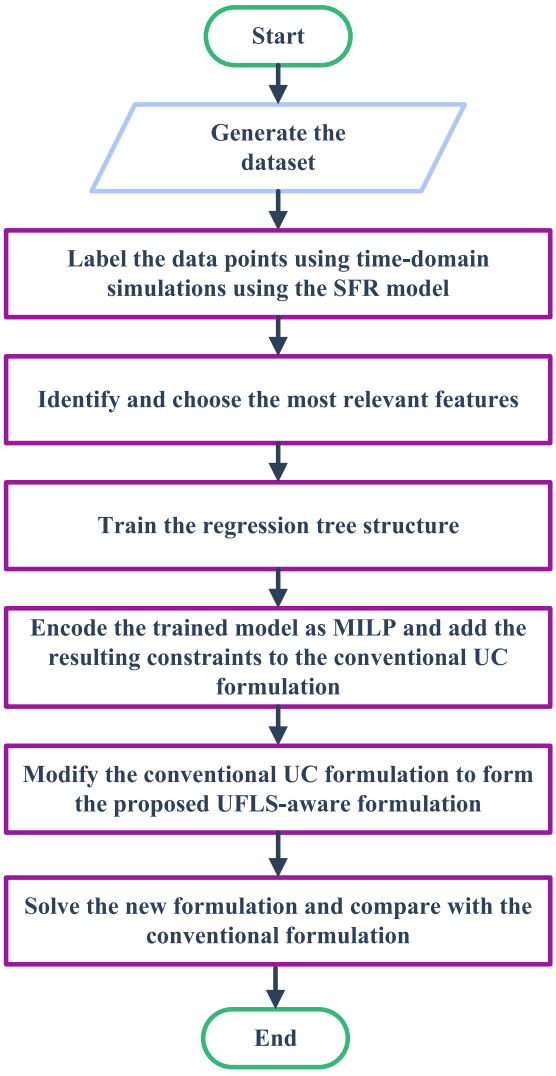

Fig. 2. Methodology framework of the paper.

Binary logic. To express minimum up-time and minimum down-time constraints, we introduce two binary variables:

$$v_{i,t} := \max\{u_{i,t} - u_{i,t-1}, 0\} = \begin{cases} 1 & \text{if } u_{i,t-1} = 0 \text{ and } u_{i,t} = 1 \\ 0 & \text{otherwise} \end{cases} \tag{4}$$

$$w_{i,t} := \max\{u_{i,t-1} - u_{i,t}, 0\} = \begin{cases} 1 & \text{if } u_{i,t-1} = 1 \text{ and } u_{i,t} = 0 \\ 0 & \text{otherwise} \end{cases} \tag{5}$$

In other words, $v_{i,t} = 1$ if and only if unit i was started at time t, and $w_{i,t} = 1$ if and only if unit i was shut down at time t.

One can show that the following linear equations uniquely determine $v_{i,t}$ and $w_{i,t}$ (provided they only take the values 0 and 1):

$$u_{i,t} - u_{i,t-1} = v_{i,t} - w_{i,t} \qquad \forall i,\ \forall t \tag{6}$$

$$v_{i,t} + w_{i,t} \le 1 \qquad \forall i,\ \forall t \tag{7}$$

This allows us to incorporate v and w into the MILP formulation.

The minimum up-time and minimum down-time constraints can then be written as follows:

$$\sum_{s=t-\mathrm{UT}_i+1}^{t} v_{i,s} \le u_{i,t} \qquad t \in \{\mathrm{UT}_i, \dots, \mathcal{T}\} \tag{8}$$

$$\sum_{s=t-\mathrm{DT}_i+1}^{t} w_{i,s} \le 1 - u_{i,t} \qquad t \in \{\mathrm{DT}_i, \dots, \mathcal{T}\} \tag{9}$$

where UT_i and DT_i are the minimum for the up-time and down-time of unit i, respectively. To understand these constraints, Eq. (8) says that if unit i was started ($v_{i,s} = 1$) at any time s between $t - \mathrm{UT}_i + 1$ and t, then unit i must be running at time t ($u_{i,t} = 1$). A similar reasoning explains Eq. (9).

Bound constraints. The minimum power generation constraint is presented in Eq. (10). Eq. (11) represents the maximum power generation constraint and ensures that the power generated plus the reserve of each online unit must be less than their corresponding maximum output.

$$p_{i,t} \ge P_i^{\min} u_{i,t} \qquad \forall i,\ \forall t \tag{10}$$

$$p_{i,t} + r_{i,t} \le P_i^{\max} u_{i,t} \qquad \forall i,\ \forall t \tag{11}$$

$P^{\min}$ is the minimum generation, and $P^{\max}$ is the maximum generation capacity of the units. In addition, the reserve provided by each unit is represented by r.

Ramp rate constraints. Eq. (12) represents the ramp-up and ramp-down constraints. These constraints ensure that the rate at which a power generation unit can increase/decrease its output in a given time interval is bounded.

$$-R_i^{\mathrm{down}} \le p_{i,t} - p_{i,t-1} \le R_i^{\mathrm{up}} \qquad \forall i,\ \forall t \tag{12}$$

R^{up} and R^{down} are the maximum ramp-up and ramp-down of generating units, respectively.

Power balance. The power balance constraint is presented in Eq. (13). This constraint ensures that the total power generated by all power generation units and RES equals the total demand at any time interval.

$$\left(\sum_i p_{i,t}\right) + g_t^w + g_t^s = D_t \qquad \forall t \tag{13}$$

The wind and solar generation are represented by g^w and g^s based on historical data. D_t is the total demand in each time interval.

RoCoF constraint. In small power systems where the total inertia is low, the RoCoF constraint is usually used, because of its simplicity and effectiveness, to ensure that the RoCoF would not exceed a critical value [39].

$$h_{\ell,t} \ge \frac{p_{\ell,t} f_0}{2\Delta f_{\mathrm{crit}}} \qquad \forall t,\ \ell \tag{14}$$

Here, h_ℓ is the weighted summation of inertia constants of online generating units, defined in Eq. (15), where $\mathcal{H}_i$ and S_i^{base} are the inertia constant and the base power of unit i respectively.

$$h_{\ell,t} := \sum_{i \ne \ell} (\mathcal{H}_i S_i^{\mathrm{base}}) \tag{15}$$

Δf_{crit} is the critical RoCoF, f_0 is the nominal frequency, and p_ℓ is power lost corresponding to the outage of unit ℓ.

Spinning reserve. The spinning reserve constraint ensures that there will be enough reserve if a generating unit is lost. Traditionally Eq. (16) is added to the UC formulation.

$$r_{\ell,t} := \sum_{i \ne \ell} r_{i,t} \ge p_{\ell,t} \qquad \forall t,\ \ell \tag{16}$$

Eq. (16) ensures that the available reserve is sufficient to endure the loss of any single unit (i.e., we enforce an N-1 security criterion). However, the distribution of the available reserve is not considered. This is critical, especially in small systems, where an outage may lead to scenarios where the available reserve is sufficient but the units providing it are not fast enough to ensure an acceptable frequency response. To address this problem, Eq. (16) can be replaced with Eq. (17) to enhance the quality of the frequency response [35]. Eq. (17)

ensures that the net power imbalance is distributed among the available units proportional to their primary frequency control speed.

$$r_{i,t} \geq \frac{\hat{K}_i u_{i,t}}{\hat{K}^s_{\ell,t}} p_{\ell,t} \qquad \forall i \neq \ell \tag{17}$$

where

$$\hat{K}^s_{\ell,t} := \sum_{i \neq \ell} \hat{K}_i u_{i,t} \tag{18}$$

and

$$\hat{K}_i := \frac{K_i}{T} \tag{19}$$

Here, T is the delivery time of each unit, and $\hat{K}_i$ is the turbine governor gain of each unit divided by its T.

In this paper, an estimation of the UFLS is incorporated into the problem to form the UFLS-aware UC formulation. The UFLS estimation details are provided in Section 2.2. For a sufficiently large outage that activates UFLS scheme, it can be argued that the reserve requirement in Eq. (17) is excessive, leading to overly conservative solutions. Therefore, to account for UFLS, we relax Eq. (17) to Eq. (20) where $p^{\text{UFLS}}_{\ell,t}$ is the estimated UFLS relating to the outage of unit ℓ at time t.

$$r_{i,t} \geq \frac{\hat{K}_i u_{i,t}}{\hat{K}^s_{\ell,t}} (p_{\ell,t} - p^{\text{UFLS}}_{\ell,t}) \qquad \forall t,\ \ell \tag{20}$$

According to the definition of $\hat{K}^s_{\ell,t}$ in Eq. (18), when substituted in Eq. (20), causes Eq. (20) to become non-linear. However, it is easy to see that Eq. (20) is equivalent to

$$\hat{K}_i (p_{\ell,t} - p^{\text{UFLS}}_{\ell,t}) \leq r_{i,t} \hat{K}^s_{\ell,t} + M(1 - u_{i,t}) \qquad \forall i \neq \ell \tag{21}$$

where M is a sufficiently big number (e.g. $M := (\max_i \hat{K}_i)(\max_i P^{\max}_i)$). This leaves us the only non-linear term to be $r_{i,t}\hat{K}^s_{\ell,t}$. Each of the resulting binary to continuous non-linear terms $r_{i,t}u_{b,t}$ can be linearized using the following set of constraints where $c_{i,b,t}$ is a positive variable representing the result of the multiplication, b is an alias index of i, and M is a sufficiently big number ($M := \max_i(P^{\max}_i - P^{\min}_i)$) [35].

$$c_{i,b,t} \leq M u_{b,t} \tag{22a}$$

$$c_{i,b,t} \leq r_{i,t} \tag{22b}$$

$$c_{i,b,t} \geq r_{i,t} - M(1 - u_{b,t}) \tag{22c}$$

2.2. UFLS estimation

The UFLS estimation method utilized here was previously developed in [37] and employs a novel regression tree structure. This method involves the generation of the dataset, effective feature selection, the learning process, and the MILP representation of the structure. Here, the key aspects of this method are presented to help better understand the framework applied. More details of these procedures can be found in [37].

2.2.1. Characteristics of the problem

Incorporating real UFLS schemes into UC formulations is complex due to various factors. The UC problem is primarily formulated as an MILP problem. On the other hand, real UFLS schemes are designed in steps that activate the relays with a preset time delay after certain thresholds are exceeded. Representing these characteristics with linear constraints that can be added to the UC problem is challenging since there is no clear relationship between the amount of shed load and the variables of the UC problem. Alternatively, data-driven methods can be employed to provide accurate UFLS estimations with a relatively simple structure and linearized constraints that can be used in the MILP formulation.

Fig. 3 presents a histogram of UFLS occurrences for all possible outages in the dataset. The employed UFLS estimation method is tailored specifically to suit the distribution and characteristics of the data in Fig. 3; considering that many incidents would not trigger the UFLS scheme (UFLS is equal to zero), and due to the step-wise activation of the UFLS scheme the data will naturally be clustered in groups (i.e., centered around specific values like 1.5 MW and 5 MW in Fig. 3). Another useful property of the tree structure for this purpose is that it can easily be represented by a set of MILP constraints, while not imposing much computational burden on the already hard-to-solve formulation of the UC problem.

2.2.2. Dataset and features

Estimating UFLS requires a comprehensive dataset consisting of features, denoted as $x \in X$, and labels, denoted as $y \in Y$. Here, features consist of various measurable quantities from the power system that aid in UFLS prediction and are accessible throughout the scheduling process. Notably, the sum of available inertia (h_ℓ), the weighted gain of the turbine-governor model ($\hat{K}^s_\ell$) that is defined in Eq. (18), lost power (p_ℓ), and the sum of available reserve (r_ℓ) after the outage of generator ℓ are identified as features for predicting UFLS.

To label the data with the values of UFLS, the SFR model is utilized. Fig. 4 illustrates the utilized SFR model, for a system comprising I generating units depicted by a simplified second-order model approximation of their turbine-governor system. The detailed model is elaborated in [40]. The parameters of the SFR model can be obtained from field tests or more detailed simulation models. However, the proposed method is not dependent on the dynamic simulation model used, and more detailed simulation models can be employed for labeling.

The generated dataset contains all viable and economical generation combinations of the system under study. The process of generating the dataset is presented in algorithm 1. First, every possible combination of the generation output of the units is considered. Then, the combinations that do not satisfy the constraints that are used in the scheduling process (e.g., power balance, reserve constraint, or maximum RoCoF) are omitted. Then, the whole set is sorted, and a reasonable number of cheaper combinations that are more likely to be the solution of the optimization problem are selected and used as the dataset [37].

Algorithm 1 Synthetic Data Generation

Inputs: $\overline{D}$, $\underline{D}$, $P^{\max}_i$, Δf_{crit}, f_0, $\mathcal{H}_i$, S^{base}_i
Output: $\mathcal{F}$: set of feasible power level vectors

$\mathcal{F} \leftarrow \emptyset$
for $\vec{p} \in \bigtimes_{i=1}^{I} \mathcal{P}_i$ **do** ▷ for all power level vectors
  for $i \in \{1, \dots, I\}$ **do** ▷ for every generator
    $u_i := 0$ if $p_i = 0$ else 1 ▷ status of unit
  end for
  $G := \sum_{i=1}^{I} p_i$ ▷ total generation
  r_ℓ ▷ reserve after outage of ℓ
  h_ℓ ▷ inertia after outage of ℓ
  if $\underline{D} \leq G \leq \overline{D}$ and $r_\ell \geq p_\ell$ and $h_\ell \geq \frac{p_\ell f_0}{2\Delta f_{\text{crit}}}$ **then** ▷ feasible?
    $\mathcal{F} \leftarrow \mathcal{F} \cup \{\vec{p}\}$ ▷ add power level vector
  end if
end for
Sort $\mathcal{F}$ ascending by the quadratic generation cost function
Keep a reasonable number of cheaper combinations and remove the rest

$\overline{D}$ and $\underline{D}$ are lower and upper bounds on yearly thermal generation (MW), i is the index of unit $\in \{1, \dots, I\}$, $\overline{P}_i$ is the capacity of unit i (MW), Δf_{crit} is critical RoCoF (Hz/s), f_0 is nominal frequency (Hz), $\mathcal{P}_i$ is the finite set of power levels of unit i including level 0 for not committed (MW), ℓ is the index of the lost unit (can be any i), $\mathcal{H}_i$ is the inertia of unit i, and S^{base}_i is the base power of unit i.

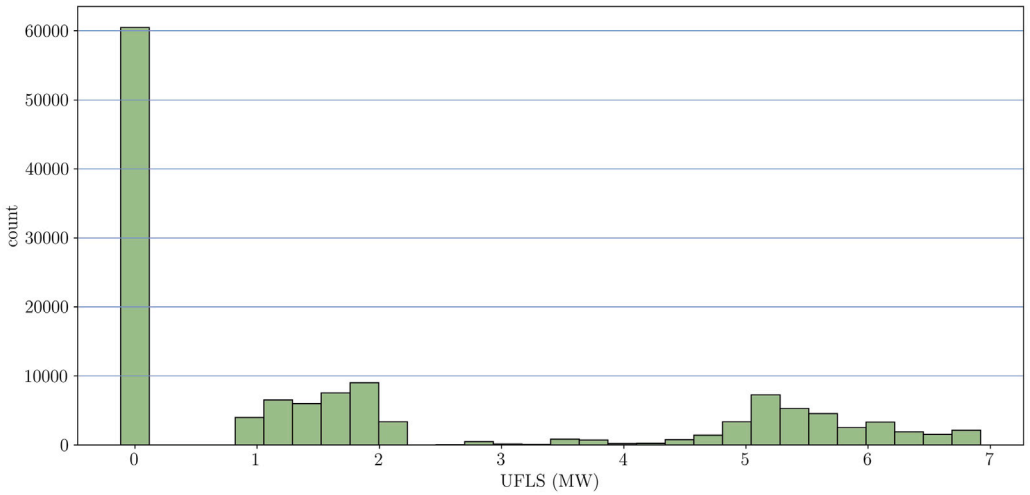

Fig. 3. Histogram of the UFLS amounts after simulation of every possible N-1 contingency in the dataset.

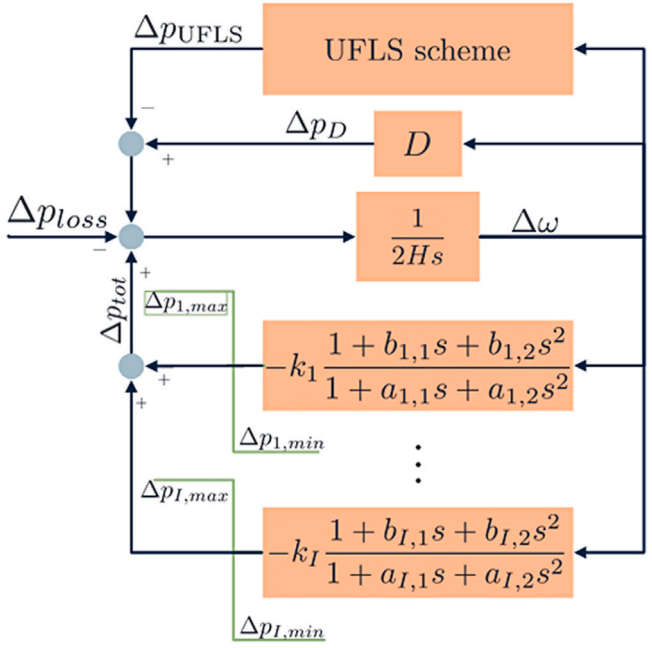

Fig. 4. SFR model [41].

2.2.3. Regression tree

The suggested regression tree utilizes logistic regression with a linear function of features to classify the UFLS predictions into two groups, and linear regression is applied within each leaf to estimate the amount of UFLS at each leaf node. A grid search is necessary to choose the threshold of each classification and to minimize the error of the local linear models. The tree structure must maintain as few cells as possible, ensuring that the MILP remains as simple as possible.

2.2.4. MILP representation

To incorporate the estimated UFLS into the UC problem, a MILP representation of the proposed tree is required. First, binary variables z_L for each leaf are defined, which are equal to 1 if the estimated UFLS falls into leaf L. Eq. (23) guarantees that each sample can belong to one leaf only.

$$\sum_{L\in\mathcal{L}} z_L = 1 \tag{23}$$

The following constraints ensure that z_L takes these values as a function of the feature vector x.

$$\hat{\beta}_0^0 + \sum_{j=1}^{J} \hat{\beta}_j^0 x_j + \underline{M} \sum_{L\in\mathcal{L}'} z_L \geq \underline{M} \tag{24a}$$

$$\hat{\beta}_0^0 + \sum_{j=1}^{J} \hat{\beta}_j^0 x_j + \overline{M} \sum_{L\in\mathcal{L}''} z_L < \overline{M} \tag{24b}$$

Where, $\hat{\beta}^{(0)}$ are the logistic regression coefficients for node N_0, and $\underline{M}$ and $\overline{M}$ are big negative and positive numbers respectively ($\overline{M} := \max(\hat{\beta}_0^0 + \sum_{j=1}^{J} \hat{\beta}_j^0 x_j)$ and $\underline{M} := \min(-\hat{\beta}_0^0 - \sum_{j=1}^{J} \hat{\beta}_j^0 x_j)$). $\mathcal{L}'$ and $\mathcal{L}''$ are the list of leaves in the right and left subtrees of the node N_0. These constraints represent the classifications that happen in each node of the resulting regression tree. The logistic regression models that are trained for each node are represented through these constraints. A similar set of constraints must be defined for each node.

After assigning binary variables, p^{UFLS} should be calculated using the linear regression models that are trained at each leaf of the regression tree. The following constraint aggregates the linear regression models and uses the binary variable z_L to make sure that only one of the models is used to estimate the amount of UFLS, as every point has to only fall into one leaf.

$$p^{\text{UFLS}} = \sum_{L\in\mathcal{L}} z_L \times \left(\alpha_0^L + \sum_{j=1}^{J} \alpha_j^L x_j\right) \tag{25}$$

Where α_j are the linear regression coefficients.

The following constraints are used to linearize Eq. (25) for each leaf L, as there are some nonlinear terms in the equation resulting from the multiplication of binary variables z_L and variables x_j that are the features of the model.

$$\alpha_0^L + \sum_{j=1}^{J} \alpha_j^L x_j - \overline{M}(1 - z_L) \leq q_L \tag{26a}$$

$$\alpha_0^L + \sum_{j=1}^{J} \alpha_j^L x_j - \underline{M}(1 - z_L) \geq q_L \tag{26b}$$

$$\overline{M} z_L \geq q_L \tag{26c}$$

$$\underline{M} z_L \leq q_L \tag{26d}$$

where q_{ℓ_e} is an auxiliary variable, $\overline{M}$ is a sufficiently big positive number ($\overline{M} := \max_L(\alpha_0^L + \sum_{j=1}^{J} \alpha_j^L x_j)$), and $\underline{M}$ is a sufficiently small negative number ($\underline{M} := \min_L(-\alpha_0^L - \sum_{j=1}^{J} \alpha_j^L x_j)$).

Finally, the linear equation for UFLS estimation can be written as:

$$p^{\text{UFLS}} = \sum_{L\in\mathcal{L}} q_L \tag{27}$$

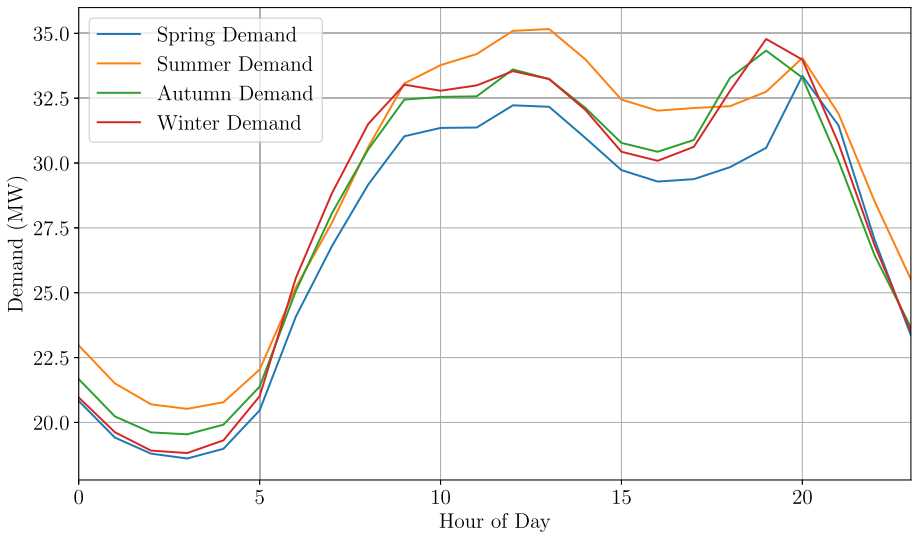

Fig. 5. Hourly demand of four seasonal days.

To conclude, Eqs. (26) and (27) are generated for each leaf and Eq. (24) are generated for each node and added to the optimization problem, along with Eq. (23), to have an estimation of UFLS in the optimization problem of scheduling generators and form the proposed UFLS-aware UC formulation.

2.3. Model definition

Two different formulations are specified for the sake of comparison and to show the effectiveness of the proposed formulation.

- Conventional UC model, in which the objective is to minimize Eq. (1) subjected to Eqs. (6)–(14) and (17).
- Proposed UFLS-aware UC model, in which the objective is minimizing Eq. (2) subjected to Eqs. (3), (6)–(14) and (21), in addition to the constraints related to the MILP representation of the proposed tree structure (Eqs. (23)–(27))

The first model features the conventional UC formulation, incorporating units' response speed. In contrast, the second model includes UFLS awareness. The numerical results of these models are compared in the following section, evaluating operation costs and costs associated with the total UFLS occurrences.

3. Results

3.1. Case study description

The simulations are performed using the model of a real island power system in Spain. The peak demand in this network is about 45.8 MW and the yearly demand is about 278.7 GWh according to recent data [42]. The synchronous generation capacity of this power system is 95.86 MW, predominantly consisting of eleven diesel generators. These diesel generators are the sole sources of inertia for the system. About 10% of the yearly demand is supplied by RES in total, and wind power generation covers about 6% [41]. This amount of RES does not currently provide inertia to the system, which significantly affects the frequency response, as the already limited amount of inertia will be lower in the presence of the RES. The technical details of the diesel generators are presented in Table 2. All the codes and obtained results are uploaded to the repository in [43].

The proposed models in Section 2.3 are solved for spring, summer, autumn, and winter sample days to confirm that the regression tree performs well with different inputs. Fig. 5 illustrates the hourly demand of these four seasonal days.

Table 2
Parameters of the Generating Units.

Unit	P^{max} (MW)	P^{min} (MW)	S^{base} (MVA)	H (s)	K (pu)	T (s)
1	3.82	2.35	5.4	1.75	20	8.26
2	3.82	2.35	5.4	1.75	20	8.26
3	3.82	2.35	5.4	1.75	20	8.26
4	4.3	2.82	6.3	1.73	20	8.26
5	6.7	3.3	9.4	2.16	20	8.26
6	6.7	3.3	9.6	1.88	20	8.26
7	11.2	6.63	15.75	2.1	20	8.26
8	11.5	6.63	14.5	2.1	20	8.26
9	11.5	6.63	14.5	2.1	20	8.26
10	11.5	6.63	14.5	2.1	20	8.26
11	21	4.85	26.82	6.5	21.25	3.28

Some realistic UFLS costs are considered. The real cost of UFLS can differ depending on the system and operator expectations. [34] uses 30k€/MW as the cost of UFLS, while in [44] the cost of shed load in mainland Europe is considered between 1.3k€/MW and 20k€/MW. Cases with different costs of UFLS are considered to show the possibility of reducing UFLS if the cost is high enough. The exact cost of UFLS varies across systems and depends on various social and technical factors. It is important to note that the actual cost of UFLS depends heavily on which loads are disconnected. Therefore, assigning different costs to each UFLS stage would make the results more realistic. However, this would raise both practical and theoretical challenges. Determining these costs precisely falls beyond the scope of this paper. Since the network mainly consists of diesel generators, the forced outage rate of generators is 2 times per year according to [45].

3.2. Regression tree training process

To effectively integrate the resulting tree into the UC problem, it is crucial that the tree has a minimal number of leaves. In the first step, incidents that do not result in UFLS are distinguished from positive amounts of UFLS. Then, a threshold is set to classify the positive instances of UFLS into two leaves. To determine the best threshold value for the split criterion in the tree structure, multiple values across a defined range were tested through a manual grid search process. This parameter plays a key role in shaping both the logistic regression and the subsequent linear regression coefficients, so fine-tuning it is critical.

Table 3
Parameters and performance metrics of the trained tree structure.

	intercept	h_ℓ	$\hat{K}^s_\ell$	p_ℓ	r_ℓ	performance
N_0	$\beta^0_0 = 0.345$	$\beta^0_1 = 0.221$	$\beta^0_2 = -0.049$	$\beta^0_3 = 7.938$	$\beta^0_4 = -0.516$	97.6% accuracy precision = 0.986 recall = 0.979 F1 score = 0.983
N_1	$\beta^1_0 = 0.300$	$\beta^1_1 = 0.013$	$\beta^1_2 = -0.027$	$\beta^1_3 = 3.904$	$\beta^1_4 = -0.384$	92.0% accuracy precision = 0.900 recall = 0.915 F1 score = 0.907
L_0	$\alpha^0_0 = 0$	$\alpha^0_1 = 0$	$\alpha^0_2 = 0$	$\alpha^0_3 = 0$	$\alpha^0_4 = 0$	MAE = 0 MSE = 0 RMSE = 0
L_1	$\alpha^1_0 = 0.0868$	$\alpha^1_1 = 0.0183$	$\alpha^1_2 = -0.000014$	$\alpha^1_3 = 0.1046$	$\alpha^1_4 = -0.532$	MAE = 0.0497 MW MSE = 0.0126 RMSE = 0.1121
L_2	$\alpha^2_0 = 0.1557$	$\alpha^2_1 = 0.0337$	$\alpha^2_2 = -0.0022$	$\alpha^2_3 = 0.8301$	$\alpha^2_4 = -0.1842$	MAE = 0.2634 MW MSE = 0.0995 RMSE = 0.3154

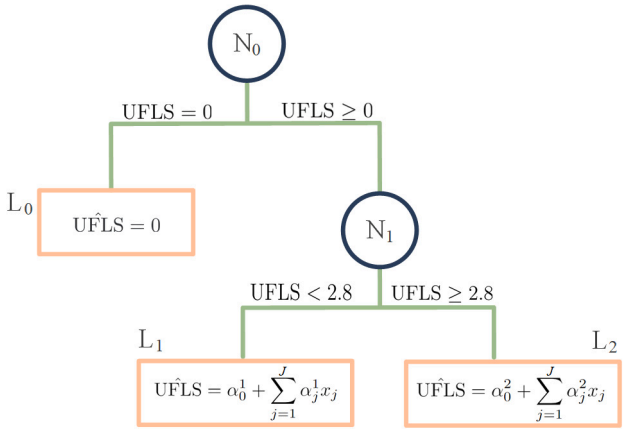

Fig. 6. The resulting trained tree structure.

At every iteration, the accuracy of the tree was evaluated. Ultimately, the threshold that delivered the most accurate results regarding the overall accuracy of the tree was selected. Finally, linear regression is performed in each of the three resulting leaves to estimate the amount of UFLS. The resulting tree structure is presented in Fig. 6. Table 3 shows the resulting parameters of logistic regression and linear regression algorithms performed. Additionally, the performance metrics of each individual model are presented to evaluate the performance of the trained structure.

3.3. Comparison of the regression tree with other regression models

In this section, the advantages of the proposed regression tree are highlighted though a comparison with different regression models. A linear regression model and three decision tree regressor models are trained using the same dataset. Table 4 shows each model's performance on a 20 percent test split of the dataset. Note that the numbers for the proposed tree structure here represent the overall performance of the regression for the whole tree and are different from the individual numbers reported in Table 3. Additionally, parameters that show the complexity of the model are presented. In Table 4 LR represents the linear regression model, DRT4 and DTR10 represent decision tree regressor models with maximum depth of 4 and 10, respectively. The metrics used for the comparison are mean absolute error (MAE), mean squared error (MSE), and root mean squared error (RMSE). The number of leaves and nodes are provided as a measure of the complexity of the model.

Table 4
Comparison of the performance and complexity of common regression models and the proposed tree structure.

model	MAE	MSE	RMSE	number of leaves	number of nodes
LR	0.7654	0.8852	0.9409	–	–
DTR4	0.5002	0.6884	0.8297	16	15
DTR10	0.4189	0.5624	0.7499	55	109
Proposed tree	0.2974	0.6304	0.7940	3	2

It is observed in Table 4 that, although being the most straightforward model, linear regression results in high amounts of error. This is trivial according to the characteristics and the distribution of the dataset as illustrated in Fig. 3. Although being more complex with a higher number of leaves and nodes, the decision tree regressor model with a maximum depth of 4 resulted in less favorable metrics than the proposed tree structure. Even when the maximum depth is increased to 10 with a very complex structure, the decision tree regressor model still has higher MAE than the proposed structure. This clearly highlights the capability of the proposed tree structure in providing an acceptable level of accuracy while keeping the structure of the model quite simple.

3.4. UFLS-aware UC results and comparison with conventional formulation

The results of the proposed UFLS-aware UC formulation are presented and compared with the base case conventional UC. The obtained results are shown in Table 5. Table 5 provides the total costs along with their percentage of variation from the base case conventional UC. Additionally, the total amounts of real UFLS happening, calculated using the SFR model along with their percentage of variation from the base case conventional UC, and the MAE of the UFLS estimation compared to the real amounts calculated with the SFR model, are presented.

According to Table 5, it can be inferred that the proposed formulation has noticeably decreased the total costs, ranging from 2% to 4.5% in this case study. Note that the total cost includes the operation cost and incurred UFLS costs, and it reflects the reduction in the UFLS amounts too. The conventional UC ensures enough headroom on the remaining units after an outage through the reserve constraint in Eq. (17), but this does not ensure the timely activation of the reserve. Although the amount of reserve is enough, UFLS can happen, making the results of the conventional UC overly conservative.

Table 5
Simulation results of the proposed and conventional formulations for four seasonal sample days.

seasonal day	C^o (€/MW)	formulation	total cost (k€)	$\sum p_{SFR}^{UFLS}$ (MW)	MAE (MW)
spring	0 €/MW	conventional UC	68.20	206.91	-
		UFLS-aware UC	66.49 (-2.51%)	234.67 (+13.42%)	0.0357
	3 k€/MW	conventional UC	68.34	206.91	-
		UFLS-aware UC	66.64 (-2.49%)	212.69 (+2.79%)	0.0431
	50 k€/MW	conventional UC	70.56	206.91	-
		UFLS-aware UC	68.70 (-2.64%)	194.25 (-6.12%)	0.0482
	100 k€/MW	conventional UC	72.92	206.91	-
		UFLS-aware UC	70.36 (-3.51%)	120.84 (-41.60%)	0.0816
summer	0 €/MW	conventional UC	70.60	235.93	-
		UFLS-aware UC	69.12 (-2.10%)	256.93 (+8.90%)	0.1497
	3 k€/MW	conventional UC	70.76	235.28	-
		UFLS-aware UC	69.30 (-2.06%)	254.10 (+8.00%)	0.1349
	50 k€/MW	conventional UC	73.29	235.28	-
		UFLS-aware UC	71.19 (-2.87%)	136.44 (-42.01%)	0.0837
	100 k€/MW	conventional UC	75.99	235.28	-
		UFLS-aware UC	72.53 (-4.54%)	127.82 (-45.69%)	0.1040
autumn	0 €/MW	conventional UC	68.91	192.79	-
		UFLS-aware UC	66.92 (-2.89%)	224.98 (+16.69%)	0.0411
	3 k€/MW	conventional UC	69.04	192.79	-
		UFLS-aware UC	67.07 (-2.86%)	217.09 (+12.60%)	0.0399
	50 k€/MW	conventional UC	71.11	192.79	-
		UFLS-aware UC	69.09 (-2.84%)	172.75 (-10.40%)	0.0567
	100 k€/MW	conventional UC	73.31	192.79	-
		UFLS-aware UC	70.81 (-3.41%)	117.94 (-38.83%)	0.0418
winter	0 €/MW	conventional UC	71.02	215.51	-
		UFLS-aware UC	69.41 (-2.27%)	230.76 (+7.09%)	0.0351
	3 k€/MW	conventional UC	71.17	215.51	-
		UFLS-aware UC	69.56 (-2.26%)	222.40 (+3.19%)	0.0352
	50 k€/MW	conventional UC	73.48	215.51	-
		UFLS-aware UC	71.44 (-2.77%)	164.39 (-23.71%)	0.0507
	100 k€/MW	conventional UC	74.94	215.51	-
		UFLS-aware UC	72.94 (-2.67%)	128.06 (-40.60%)	0.0754

The proposed UFLS-aware UC formulation has lowered the reserve requirement by utilizing the estimated amount of UFLS. A sensitivity analysis is performed to observe the effects of the cost associated with the UFLS. Based on the results presented in Table 5, it can be observed that the costs increase with higher C^0, but the total UFLS that is expected to happen will decrease. This indicates that the operator can choose to prioritize minimizing the UFLS with high UFLS costs or prioritize minimizing operation costs with lower UFLS costs. With the proper evaluation of the UFLS costs, the proposed formulation can decrease both the operation cost and the amount of UFLS compared to the conventional UC formulation. In this study, for post-outage UFLS costs of 0 and 3 k€/MW, the operation costs are lower, but this will result in overall higher amounts of UFLS, compared to the conventional UC formulation. By contrast, for post-outage UFLS costs of 50 k€/MW and 100 k€/MW, the proposed formulation has successfully decreased both the operation costs and the total UFLS that will happen after outages, but the operation costs are higher than previous scenarios.

Day-ahead scheduled generation of the base case conventional UC problem is shown in Fig. 7(a). Fig. 7(b) shows scheduling results of the proposed UFLS-aware UC formulation for a sample day in autumn when the post-outage UFLS cost is 50 k€/MW. Fig. 7 illustrates that cheaper commitment combinations are allowed in the proposed formulation. Although expensive, unit i_8 generates power in the conventional formulation to satisfy the reserve requirement. In contrast, in the proposed formulation, unit i_8 is turned off and units i_3 and i_4 keep generating as a cheaper alternative since the reserve requirement is lower.

The available reserve of each unit, the biggest online unit (BOU) in each hour, and the amount of UFLS that occurs corresponding to the biggest outage possible in each hour for a sample day in autumn in three different scenarios are shown in Fig. 8. Fig. 8(a) shows the available reserve in the conventional formulation. The available reserve and UFLS estimations of the proposed UFLS-aware UC when the post-outage UFLS costs are 0 and 50 k€ are illustrated in Fig. 8(b) and Fig. 8(c), respectively. Fig. 8 highlights the substantial differences between the proposed formulation and the conventional UC. Comparing Fig. 8(a) and Fig. 8(b), it is observed that the estimated amount of UFLS corresponding to the biggest outage can significantly contribute to the amount of provided reserve for this outage, resulting in lower amounts of reserve needed. Hence, the operation cost will decrease. In contrast to Fig. 8(b), Fig. 8(c) exemplifies that with higher costs associated with the UFLS, lower amounts of UFLS will occur. However, there are still benefits in utilizing them to compensate for the reserve requirement in big outages in some of the time intervals.

Fig. 9 provides a more detailed breakdown of every possible outage in the sample day of autumn and hour 22. The amount of available reserve after each outage, the amount of UFLS, and the required reserve of each outage (RRO) are illustrated in Fig. 9. The outage of every generating unit is examined. Some outages do not lead to UFLS, but some do. It is observed that in the event of unit number 7 outage, which is the biggest online generating unit, the inevitable amount of UFLS is utilized as a source of reserve.

To give a more detailed comparison of the frequency responses, time-domain SFR simulations are compared for the proposed method when C^o = 50 k€/MW and the conventional UC in terms of different key performance indexes (KPIs) in Table 6. The improvements in the UFLS amounts are evident both in comparing the total summation of UFLS amounts and the amount of resulting UFLS per outage. Similarly, the minimum frequency nadir and maximum frequency amounts are consistently improved. Note that although the average frequency nadirs over the total outages are higher, they remain within the acceptable thresholds, as the minimum nadir is always lower in the conventional formulation.

The estimated amounts of the UFLS are compared with those calculated using the mentioned SFR model, to show the errors associated with the proposed estimation method. Fig. 10 shows a histogram of errors between the estimated amount of UFLS, using the data-driven

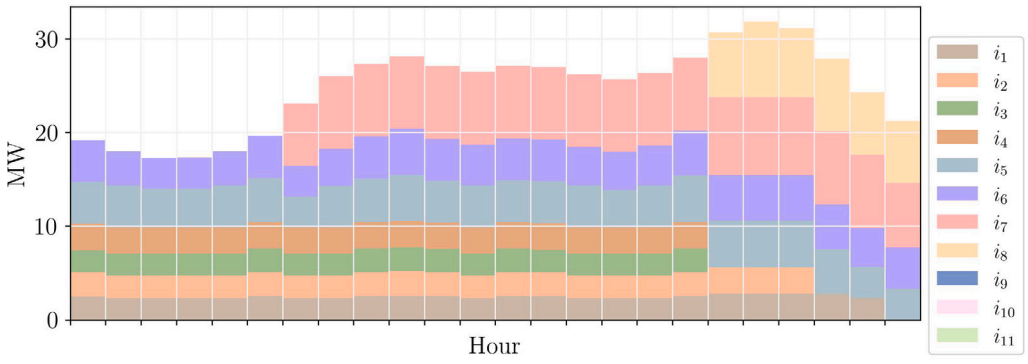

(a) Day-ahead scheduled generation (Conventional UC, autumn)

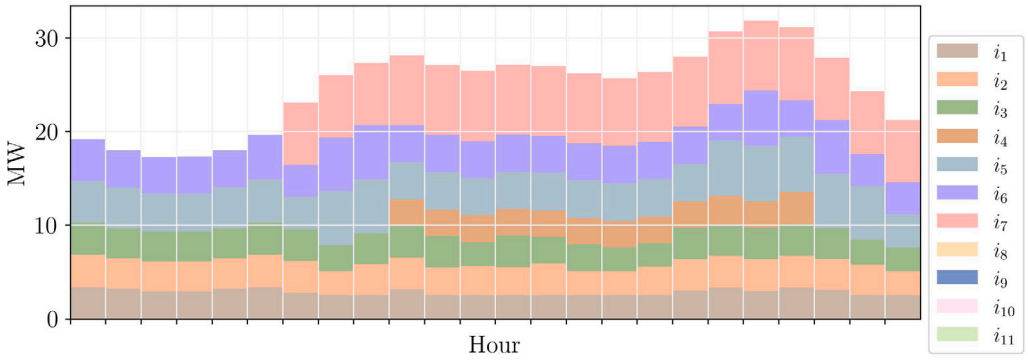

(b) Day-ahead scheduled generation ($C^o = 50$ k€/MW, autumn)

Fig. 7. Day-ahead scheduled generation of the units.

Table 6
Time-domain SFR simulation KPIs for the proposed and conventional formulations.

sample day	formulation	$\sum p_{\text{SFR}}^{\text{UFLS}}$ (MW)	$\frac{\sum p_{\text{SFR}}^{\text{UFLS}}}{n_{\text{outage}}}$ (MW)	$\frac{\sum f_{\text{nadir}}}{n_{\text{outage}}}$ (Hz)	$f_{\text{nadir}}^{\text{min}}$ (Hz)	f^{max} (Hz)
spring	conventional	206.91	1.43	−1.13	−1.96	50.25
	proposed	194.25	1.37	−1.22	−1.87	50.14
summer	conventional	235.28	1.63	−1.12	−1.94	50.31
	proposed	134.26	0.84	−1.08	−1.87	50.17
autumn	conventional	192.79	1.27	−1.07	−1.85	50.26
	proposed	172.75	1.15	−1.14	−1.84	50.16
winter	conventional	215.51	1.43	−1.09	−1.95	50.24
	proposed	164.39	1.06	−1.12	−1.86	50.19

constraints in the UFLS-aware UC formulation, and the amount of UFLS simulated by using the SFR model for all possible outages. It can be observed that the data-driven constraints have successfully been able to estimate UFLS in most of the cases. Additionally, the few major errors represent the errors associated with the accuracy of the tree structure as expected. The MAE presented in Table 5 elaborates on the proposed formulation's acceptable accuracy concerning the tree structure's accuracy.

3.5. Comparison with analytical method

In this section, a detailed comparison between the proposed methodology and the analytical approach provided in [35] highlights the benefits of the proposed methodology. Fig. 11 illustrates the post-contingency frequency performance corresponding to every possible outage in the four sample days for both methods when $C^o = 50$ k€/MW. As expected, the UFLS scheme is activated when necessary to maintain stability. Fig. 11 shows that the system's security has not been jeopardized in every possible contingency. Concluding that the operation points of the proposed formulation are secured completely through the UFLS schemes.

Fig. 11 compares the post-contingency frequency performance of the proposed method with the analytical method. It can be observed that the proposed method has consistently resulted in better frequency response in terms of various KPIs. The numerical results of the time-domain simulations KPIs and operation costs are provided in Table 7 for both methods.

Comparing the numbers in Table 7 for the two methods, it is observed that the proposed method outperforms the analytical method in almost every KPI in different loading conditions of the analyzed

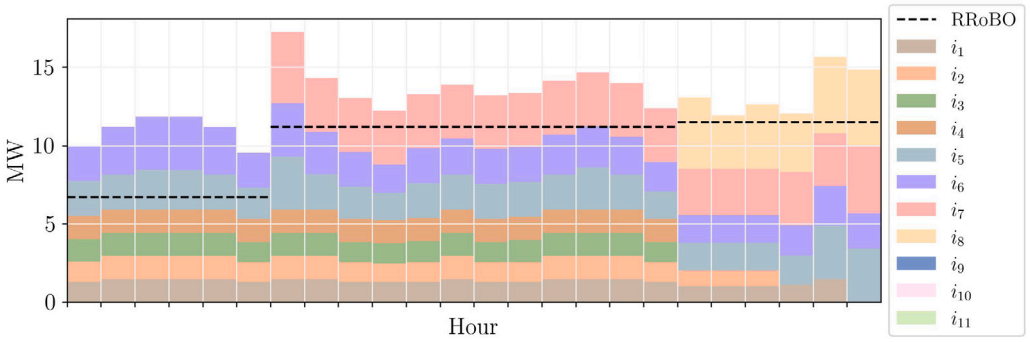

(a) Scheduled available reserve (Conventional UC, autumn)

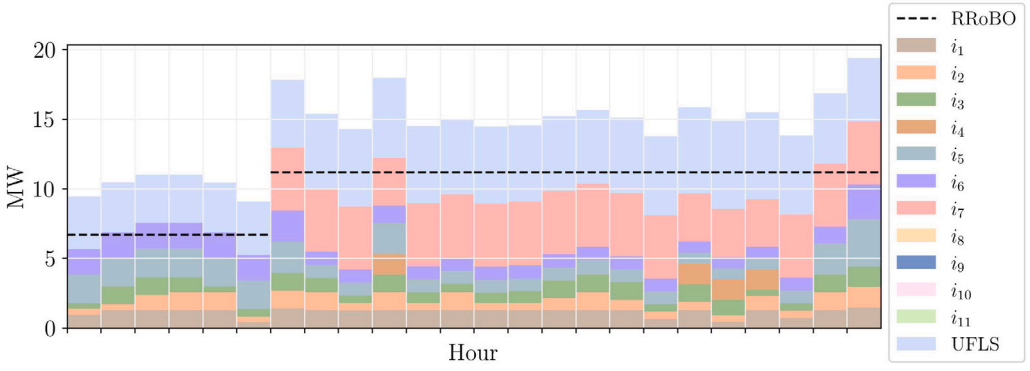

(b) Scheduled available reserve ($C^o = 0$ €/MW, autumn)

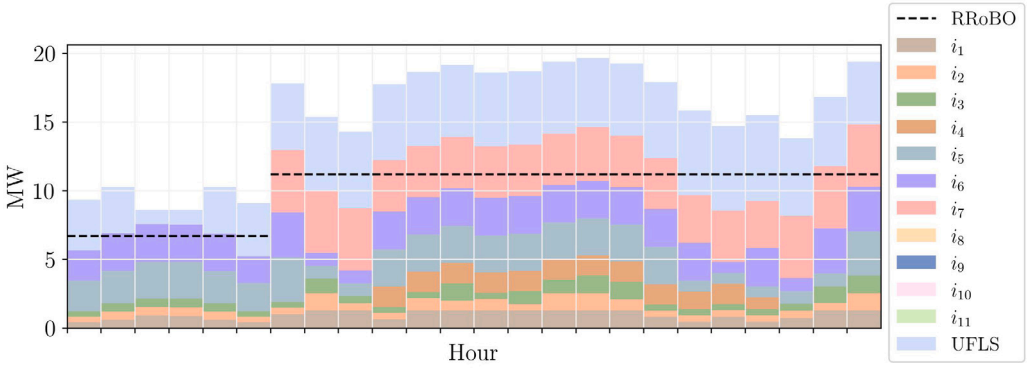

(c) Scheduled available reserve ($C^o = 50$ k€/MW, autumn)

Fig. 8. Scheduled available reserve of the units.

Table 7
Time-domain SFR simulation KPIs for the proposed and analytical method.

sample day	method	$\sum p_{\text{SFR}}^{\text{UFLS}}$ (MW)	$\frac{\sum p_{\text{SFR}}^{\text{UFLS}}}{n_{\text{outage}}}$ (MW)	$\frac{\sum f_{\text{nadir}}}{n_{\text{outage}}}$ (Hz)	$f_{\text{nadir}}^{\min}$ (Hz)	$f^{\max}$ (Hz)	$c^{\text{g}} + c^{\text{suc}}$ (k€)
spring	analytical	199.20	1.38	−1.21	−1.96	50.26	68.18
	proposed	194.25	1.37	−1.22	−1.87	50.14	66.54
summer	analytical	209.27	1.45	−1.20	−1.94	50.27	70.20
	proposed	134.26	0.84	−1.08	−1.87	50.17	69.78
autumn	analytical	176.49	1.19	−1.16	−1.87	50.32	68.88
	proposed	172.75	1.15	−1.14	−1.84	50.16	67.20
winter	analytical	198.06	1.36	−1.18	−1.95	50.27	70.73
	proposed	164.39	1.06	−1.12	−1.86	50.19	69.62

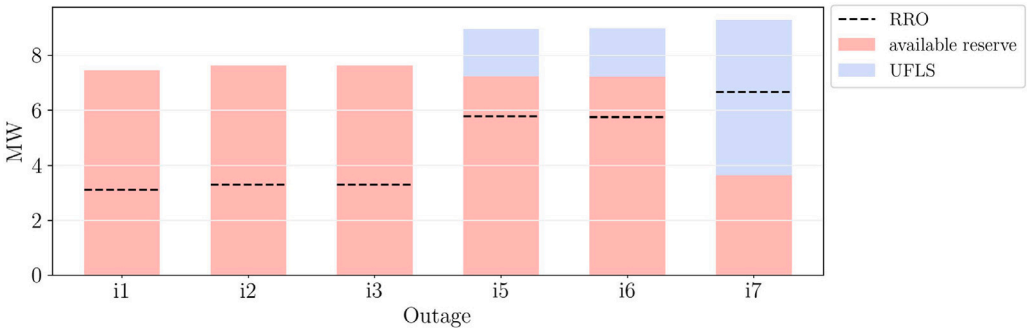

Fig. 9. Reserve and UFLS illustration of each possible outage on hour 22 (C^o = 50 k€/MW, autumn).

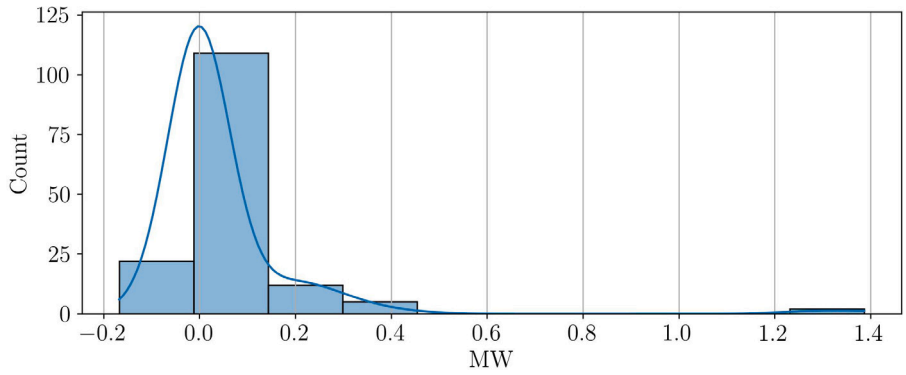

Fig. 10. Histogram of errors between estimated and simulated amount of UFLS (C^o = 50 k€/MW, autumn).

sample days. Note that although maximum RoCoF is an important KPI, it is not included here since Eq. (14) limits this amount to a threshold for both methods and the resulting number will be the same for both methods.

Moreover, the operation costs in the proposed formulation are consistently lower than those in the analytical method. In other words, the proposed formulation is capable of having a more accurate estimation of the possible UFLS amounts and through them, not only gives cheaper solutions to the UC problem, but also results in more favorable post-contingency frequency performance and lower total UFLS amounts compared to the analytical formulation.

4. Conclusion

In this paper, a UFLS-aware UC formulation is presented that enables co-optimization of operation costs and UFLS costs. To achieve this, a previously developed data-driven estimation of UFLS is employed and presented as a set of linear constraints. According to the fact that for sufficiently large outages in small IPS, UFLS is inevitable, co-optimizing operation and UFLS allows the operator to schedule less reserve, given the fact that they are aware of the amount of UFLS through the proposed formulation.

Simulation results show that the proposed formulation leads to lower operation costs. Different UFLS costs are considered to illustrate that with proper adjustment, the operator can tune their desired level of conservativeness and balance the trade-off between operation costs and the amount of UFLS. The simulation is performed on four days of the year to show its effectiveness for different data points.

CRediT authorship contribution statement

Miad Sarvarizadeh: Visualization, Methodology, Conceptualization, Writing – original draft, Software, Data curation, Validation, Investigation. **Mohammad Rajabdorri:** Writing – review & editing, Software, Data curation, Supervision, Formal analysis, Validation, Methodology, Conceptualization. **Enrique Lobato:** Supervision, Funding acquisition, Validation, Project administration, Conceptualization, Writing – review & editing, Resources, Formal analysis. **Lukas Sigrist:** Writing – review & editing, Methodology, Conceptualization, Supervision, Formal analysis, Validation, Funding acquisition. **Behzad Kazemtabrizi:** Validation, Writing – review & editing, Conceptualization, Methodology. **Matthias Troffaes:** Methodology, Validation, Writing – review & editing, Conceptualization.

Declaration of competing interest

The authors declare that they have no known competing financial interests or personal relationships that could have appeared to influence the work reported in this paper.

Acknowledgments

This research has been funded by grant PID2022-141765OB-I00 funded by MCIN/AEI/ 10.13039/501100011033 and by “ERDF A way of making Europe”.

Data availability

We have shared the link to the codes used in the manuscript.

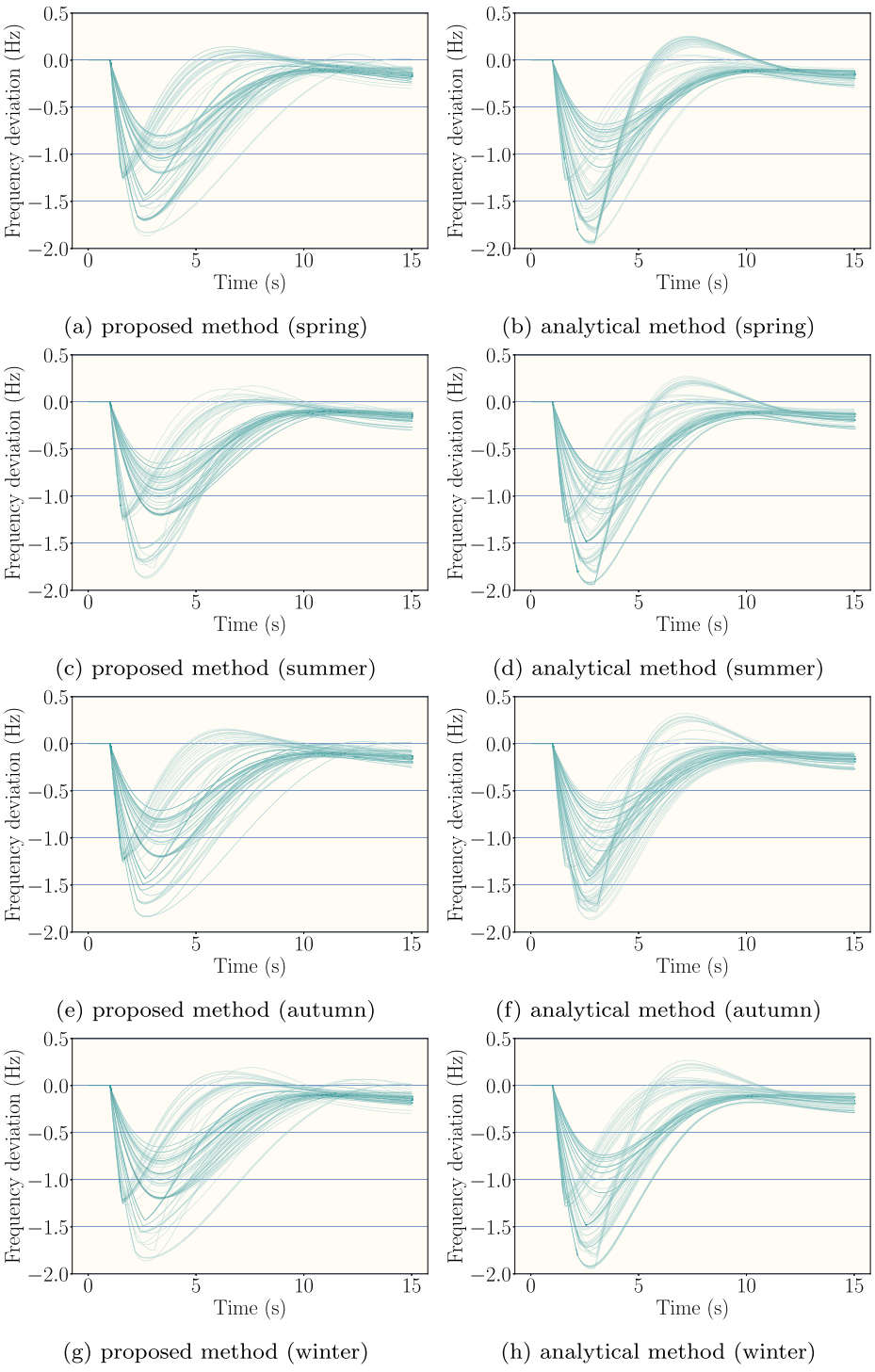

Fig. 11. Post-contingency frequency comparison of the proposed and analytical method.

References

[1] Shazon MNH, Nahid-Al-Masood, Jawad A. Frequency control challenges and potential countermeasures in future low-inertia power systems: A review. Energy Rep 2022;8:6191–219. http://dx.doi.org/10.1016/j.egyr.2022.04.063.

[2] Hoke A, Gevorgian V, Shah S, Koralewicz P, Kenyon RW, Kroposki B. Island power systems with high levels of inverter-based resources: Stability and reliability challenges. IEEE Electrification Mag 2021;9:74–91. http://dx.doi.org/10.1109/MELE.2020.3047169.

[3] Sigrist L, Lobato E, Echavarren F, Egido I, Rouco L. Island power systems. CRC Press; 2016.

[4] Mancarella P, Billimoria F. The fragile grid: The physics and economics of security services in low-carbon power systems. IEEE Power Energy Mag 2021;19(2):79–88. http://dx.doi.org/10.1109/MPE.2020.3043570.

[5] Rabbanifar P, Amjady N. Frequency-constrained unit-commitment using analytical solutions for system frequency responses considering generator contingencies. IET Gener Transm Distrib 2020;14(17):3548–60. http://dx.doi.org/10.1049/iet-gtd.2020.0097, arXiv:https://ietresearch.onlinelibrary.wiley.com/doi/pdf/10.1049/iet-gtd.2020.0097, URL https://ietresearch.onlinelibrary.wiley.com/doi/abs/10.1049/iet-gtd.2020.0097.

[6] Zhou B, Jiang R, Shen S. Frequency stability-constrained unit commitment: Tight approximation using Bernstein polynomials. IEEE Trans Power Syst 2023.

[7] Tuo M, Li X. Security-constrained unit commitment considering locational frequency stability in low-inertia power grids. IEEE Trans Power Syst 2022.

[8] Zhang Y, Guo Q, Zhou Y, Sun H. Frequency-constrained unit commitment for power systems with high renewable energy penetration. Int J Electr Power Energy Syst 2023;153:109274.
[9] Qi X, Zhao T, Liu X, Wang P. Three-stage stochastic unit commitment for microgrids towards frequency security via renewable energy deloading. IEEE Trans Smart Grid 2023.
[10] Li K, Ai X, Fang J, Cui S, Feng Y, Liu D, et al. Frequency security constrained robust unit commitment for sufficient deployment of diversified frequency support resources. IEEE Trans Ind Appl 2023.
[11] Shen Y, Wu W, Wang B, Yang Y, Lin Y. Data-driven convexification for frequency nadir constraint of unit commitment. J Mod Power Syst Clean Energy 2023;11(5):1711–7. http://dx.doi.org/10.35833/MPCE.2021.000734.
[12] Sang L, Xu Y, Yi Z, Yang L, Long H, Sun H. Conservative sparse neural network embedded frequency-constrained unit commitment with distributed energy resources. IEEE Trans Sustain Energy 2023;14(4):2351–63. http://dx.doi.org/10.1109/TSTE.2023.3268140.
[13] Liu L, Hu Z, Wen Y, Ma Y. Modeling of frequency security constraints and quantification of frequency control reserve capacities for unit commitment. IEEE Trans Power Syst 2023.
[14] Xu D, Wu Z, Liu Y, Zhu L. Enhancing frequency security for renewable-dominated power systems via distributionally robust frequency constrained unit commitment. Electr Power Syst Res 2025;239:111078.
[15] Shen Y, Wu W, Wang B, Sun S. Optimal allocation of virtual inertia and droop control for renewable energy in stochastic look-ahead power dispatch. IEEE Trans Sustain Energy 2023;14(3):1881–94.
[16] Zuo Y, Frigo G, Derviškadić A, Paolone M. Impact of synchrophasor estimation algorithms in ROCOF-based under-frequency load-shedding. IEEE Trans Power Syst 2020;35(2):1305–16. http://dx.doi.org/10.1109/TPWRS.2019.2936277.
[17] Skrjanc T, Mihalic R, Rudez U. A systematic literature review on under-frequency load shedding protection using clustering methods. Renew Sustain Energy Rev 2023;180:113294.
[18] Ghaderi Darebaghi M, Amraee T. Dynamic multi-stage under frequency load shedding considering uncertainty of generation loss. IET Gener Transm Distrib 2017;11(13):3202–9. http://dx.doi.org/10.1049/iet-gtd.2016.0751, arXiv:https://ietresearch.onlinelibrary.wiley.com/doi/pdf/10.1049/iet-gtd.2016.0751, URL https://ietresearch.onlinelibrary.wiley.com/doi/abs/10.1049/iet-gtd.2016.0751.
[19] Amraee T, Darebaghi MG, Soroudi A, Keane A. Probabilistic under frequency load shedding considering RoCoF relays of distributed generators. IEEE Trans Power Syst 2017;33(4):3587–98.
[20] Laghari J, Mokhlis H, Karimi M, Bakar AHA, Mohamad H. A new under-frequency load shedding technique based on combination of fixed and random priority of loads for smart grid applications. IEEE Trans Power Syst 2014;30(5):2507–15.
[21] Lobato E, Rajabdorri M, Sigrist L, Egido I, Ortega A. Robust optimal design of UFLS schemes in island power systems. Sustain Energy Grids Netw 2024;101434.
[22] Ahsan MQ, Chowdhury AH, Ahmed SS, Bhuyan IH, Haque MA, Rahman H. Technique to develop auto load shedding and islanding scheme to prevent power system blackout. IEEE Trans Power Syst 2011;27(1):198–205.
[23] Zhang L, Zhong J. UFLS design by using f and integrating df/dt. In: 2006 IEEE PES power systems conference and exposition. IEEE; 2006, p. 1840–4.
[24] Luo Z, Liu H, Wang N, Zhao T, Tian J. Optimal adaptive decentralized under-frequency load shedding for islanded smart distribution network considering wind power uncertainty. Appl Energy 2024;365:123162.
[25] Sun M, Liu G, Popov M, Terzija V, Azizi S. Underfrequency load shedding using locally estimated RoCoF of the center of inertia. IEEE Trans Power Syst 2021;36(5):4212–22.
[26] Baškarad T, Holjevac N, Kuzle I, Ivanković I. Dynamically adaptive method for under frequency load shedding protection scheme reconfiguration. Electr Power Syst Res 2022;207:107823.
[27] Xu B, Paduani V, Xiao Q, Song L, Lubkeman D, Lu N. Under-frequency load shedding for power reserve management in islanded microgrids. IEEE Trans Smart Grid 2024.
[28] Sodin D, Ilievska R, Čampa A, Smolnikar M, Rudez U. Proving a concept of flexible under-frequency load shedding with hardware-in-the-loop testing. Energies 2020;13(14):3607.
[29] Darbandsari A, Amraee T. Under frequency load shedding for low inertia grids utilizing smart loads. Int J Electr Power Energy Syst 2022;135:107506.
[30] Zhang Y, Cui H, Liu J, Qiu F, Hong T, Yao R, et al. Encoding frequency constraints in preventive unit commitment using deep Learning With Region-of-interest active sampling. IEEE Trans Power Syst 2022;37(3):1942–55. http://dx.doi.org/10.1109/TPWRS.2021.3110881.
[31] Lai C-Y, Liu C-W. A scheme to mitigate generation trip events by ancillary services considering minimal actions of UFLS. IEEE Trans Power Syst 2020;35(6):4815–23. http://dx.doi.org/10.1109/TPWRS.2020.2993449.
[32] Teng F, Strbac G. Full stochastic scheduling for low-carbon electricity systems. IEEE Trans Autom Sci Eng 2017;14(2):461–70. http://dx.doi.org/10.1109/TASE.2016.2629479.
[33] Yuan Y, Liu Z, Chen Z, Hoej Jensen K, Popov M. Quantifying frequency containment reserve using cross-entropy frequency-constrained contingency-state-analysis model. Int J Electr Power Energy Syst 2023;145:108705. http://dx.doi.org/10.1016/j.ijepes.2022.108705, URL https://www.sciencedirect.com/science/article/pii/S0142061522007013.
[34] O'Malley C, Badesa L, Teng F, Strbac G. Probabilistic scheduling of UFLS to secure credible contingencies in low inertia systems. IEEE Trans Power Syst 2022;37(4):2693–703. http://dx.doi.org/10.1109/TPWRS.2021.3124423.
[35] Rajabdorri M, Rouco A, Sigrist L, Lobato E. Unit commitment with analytical under-frequency load-shedding constraints for island power systems. IEEE Access 2024;12:72337–44. http://dx.doi.org/10.1109/ACCESS.2024.3401854.
[36] Rajabdorri M, Lobato E, Sigrist L. Robust frequency constrained uc using data driven logistic regression for island power systems. IET Gener Transm Distrib 2022;16(24):5069–83. http://dx.doi.org/10.1049/gtd2.12658, arXiv:https://ietresearch.onlinelibrary.wiley.com/doi/pdf/10.1049/gtd2.12658, URL https://ietresearch.onlinelibrary.wiley.com/doi/abs/10.1049/gtd2.12658.
[37] Rajabdorri M, Troffaes MC, Kazemtabrizi B, Sarvarizadeh M, Sigrist L, Lobato E. Data-driven estimation of the amount of under frequency load shedding in small power systems. Eng Appl Artif Intell 2025;139:109617.
[38] Simoglou CK, Biskas PN, Bakirtzis AG. Optimal self-scheduling of a thermal producer in short-term electricity markets by MILP. IEEE Trans Power Syst 2010;25(4):1965–77. http://dx.doi.org/10.1109/TPWRS.2010.2050011.
[39] Liu J, Wang C, Zhao J, Bi T. Rocof constrained unit commitment considering spatial difference in frequency dynamics. IEEE Trans Power Syst 2024;39(1):1111–25. http://dx.doi.org/10.1109/TPWRS.2023.3240776.
[40] Sigrist L, Lobato E, Echavarren FM, Egido I, Rouco L. Island power systems. 2016, p. 1–272. http://dx.doi.org/10.1201/9781315368740.
[41] Rajabdorri M, Kazemtabrizi B, Troffaes M, Sigrist L, Lobato E. Inclusion of frequency nadir constraint in the unit commitment problem of small power systems using machine learning. Sustain Energy Grids Netw 2023;36:101161. http://dx.doi.org/10.1016/j.segan.2023.101161, URL https://www.sciencedirect.com/science/article/pii/S2352467723001698.
[42] García SS. Perspectives of marine renewable energies in the Canary Islands Canary Islands Institute of Technology International Meeting on Marine Renewable Energy.
[43] Sarvarizadeh M. Under frequency load shedding aware unit commitment in island power systems. 2024, http://dx.doi.org/10.5281/zenodo.14074731.
[44] ACER J. Study on the estimation of the value of lost load of electricity supply in Europe. 2018.
[45] Survey of reliability and availability information for power distribution, power generation, and heating, ventilating & air conditioning (hvac) components for commercial, industrial, and utility installations contents. Tech. rep. TM 5-698-5, Department of the Army; 2006, URL https://www.wbdg.org/FFC/ARMYCOE/COETM/tm_5_698_5.pdf.